International Journal on Recent and Innovation Trends in Computing and Communication
ISSN: 2321-8169 Volume: 11 Issue: 2
DOI: https://doi.org/10.17762/ijritcc.v11i2.6132
***Article Received**: 22 December 2022 **Revised**: 08 January 2023 **Accepted**: 26 January 2023*

Optimized Deep Belief Neural Network for Semantic Change Detection in Multi-Temporal Image

L. Ashok Kumar[1], Dr. M. R. Ebenezar Jebarani[2], Dr. V. Gokula Krishnan[3]
[1]Research Scholar, School of Electrical and Electronics Engineering
Sathyabama Institute of Science and Technology
Chennai, Tamil Nadu, India
e-mail: ashokkumarsathphd@gmail.com
[2]Associate Professor, School of Electrical and Electronics Engineering
Sathyabama Institute of Science and Technology
Chennai, Tamil Nadu, India
e-mail: ebenezarjebarani.ece@sathyabama.ac.in
[3]Professor, Department of CSE, Saveetha School of Engineering
Saveetha Institute of Medical and Technical Sciences
Thandalam, Chennai, Tamil Nadu, India
e-mail: gokul_kris143@yahoo.com

Abstract— Nowadays, a massive quantity of remote sensing images is utilized from tremendous earth observation platforms. For processing a wide range of remote sensing data to be transferred based on knowledge and information of them. Therefore, the necessity for providing the automated technologies to deal with multi-spectral image is done in terms of change detection. Multi-spectral images are associated with plenty of corrupted data like noise and illumination. In order to deal with such issues several techniques are utilized but they are not effective for sensitive noise and feature correlation may be missed. Several machine learning-based techniques are introduced to change detection but it is not effective for obtaining the relevant features. In other hand, the only limited datasets are available in open-source platform; therefore, the development of new proposed model is becoming difficult. In this work, an optimized deep belief neural network model is introduced based on semantic modification finding for multi-spectral images. Initially, input images with noise destruction and contrast normalization approaches are applied. Then to notice the semantic changes present in the image, the Semantic Change Detection Deep Belief Neural Network (SCD-DBN) is introduced. This research focusing on providing a change map based on balancing noise suppression and managing the edge of regions in an appropriate way. The new change detection method can automatically create features for different images and improve search results for changed regions. The projected technique shows a lower missed finding rate in the Semantic Change Detection dataset and a more ideal rate than other approaches.

Keywords- Multitemporal, Multi-spectral, Deep Belief Neural Network, Jellyfish model, Contrast Normalization, Gaussian Filter.

I. INTRODUCTION

The sustainable development of human society requires a comprehensive understanding of global change. The global change-based analysis is nowadays significant for effective environmental monitoring that helps to analyze the land based natural effects. For this analysis, the effective environmental monitoring is sufficient in terms short- and long-term observations to detect any change in land surface [1], due to the reconstituted property of the Polar field. Thus, multi-temporal remote sensing images are a significant data source for detecting changes in land surface over large geographical areas, gradually reducing the need for traditional field investigation [2]. So far, changes of the land surface are detected by utilizing the significant data source called multi-temporal remote sensing images in a wide geographical area, and the requirement for conventional field researches is progressively decreased. Here, the most important thing is change detection (CD) and it is described as the detecting operation of changes which is obtained among two or more images that are based on the image properties [5]. The image property's differences such as texture, shape, and value of pixel radiance are can be interconnected to the changes on the ground at various satellite remark times [3]. Still, the image properties may be impacted by some external features such as the condition of sensors, seasonal effects, the difference in environmental conditions, and variation of illumination [6].

In recent years, vast number of academic scholars are interested in the semantic change detection technique due to its extensive utilization in various fields such as urban environmental survey, urban planning and constructions, disaster monitoring and evaluation, acquisition of extended change information, land use, etc. [7]. The advancement is required in CDs technologies for enabling an automated change detecting based on obtaining multi-temporal images utilized

International Journal on Recent and Innovation Trends in Computing and Communication
ISSN: 2321-8169 Volume: 11 Issue: 2
DOI: https://doi.org/10.17762/ijritcc.v11i2.6132
***Article Received**: 22 December 2022 **Revised**: 08 January 2023 **Accepted**: 26 January 2023*

with remote sensing satellite systems [8]. The currently applicable technique for detecting the changes is generally categorized as pixel based, object based, and deep learning-based approach [4]. Moreover, the possibility of quality-based issues arise is high while process change detection based on several images. Therefore, the accuracy of the results also affected. However, the image of the difference usually comprises a great sum of false-changed districts in which the brightness changes, noise corruption, etc. occurs [9]. Moreover, the other considerable challenges are distinguishing the really changed regions and falsely changed region. It is significant for providing the appropriate system for dealing quality issues based on different images to distinguish the exact change [10]. The modern computer vision technologies and image processing technology-based researches are focusing on enabling the effective change detection to provide considerable benefits in terms of quality enhanced images [20].

With the development of soft computing technologies in change detection approach, the three considerable factions are really needed to focus. At first, the role of hardware components is highly significant for processing massive calculation but the machine learning is cheaper and effective [11]. Second, the novelty should be focused for providing new model. The third factor is data utilization is increasing for working with machine learning technique. Several techniques are nowadays introduced for dealing with multi-temporal aerial images that including deep learning technique, machine learning, and optimization [12]. Here, some machine learning techniques that are applied to change detection mechanism are provided namely SVM, Deep Neural Network (DNN), Bayesian Network, Artificial Neural Network (ANN). These machine learning are utilized to change detection based on satellite-based images but lacks. The sematic climate change detection is essential task which achieved with the assistance of machine learning algorithms. The deep learning process is enabled by initiating the deep learning procedure in the machine learning algorithms [13]. Many optimization algorithms are available to enhance the process of machine learning and deep learning algorithms such as Spider Monkey Optimization (SMO) respectively [14]. These algorithms are utilized to improve the process of the classification technique for achieving efficient sematic climate change detection. The main contribution and organization of the work is presented follows,

- As a means of resolving the categorical ambiguity brought on by asymmetric changes Detection (SCD) based Deep belief Neural Network (DBN) is presented here.
- A large-scale semantic change detection dataset is used to better train deep models and as a new benchmark for the change detection issue, and this is used to verify the validity of the suggested approach. This SECOND also allows us to differentiate between previously defined land-cover classes in newly developed locations.

The remaining part of the paper is prearranged as shadows. Section 2 provides the related work of semantic change detection. The further section 3 labels about motivation of the study. The section 4 provides the detail description of the projected semantic change detection. The proposed method is implemented and results are presented in section 5. To conclude, section 6 accomplishes the document.

II. RELATED WORKS

This section comprises a discussion about the works that have more deeply prejudiced this work. Some of the works are reread in this section.

Defeng Peng et al., [15] have presented a technique is called Unit ++ that is based on encoder-decoder based on architecture with sematic segmentation based on annotated datasets. Initially, a modified unit++ network is carried out based on co-recorded images. The modified unit ++ could provide high spatial accuracy. Then, this model is applied based on fusion strategy of multi-side output with combine conversion map based on different scientific approach. The final transformation map based on high accuracy. Finally, CD based approach provides high resolution (VHR) based on satellite image datasets. Likao Mau et al., [16] have provided the novel approach based on Recurrent Convulsive Neural Network (Re-CNN) based on multi-spectral images for diagnosing changes. With this method, rich spectral-spatial characteristics could provide by former, while the latter effectually analyzed the temporal dependence in bi-temporal images. It has three considerable features such as it can be calculated separately. Second, it provides default harness spatial information. The third is easy to learn multi-temporal image's temporal dependencies. Likewise, Farnam Samadi et al., [17] have projected a novel deep learning based on Deep Belief Network (DBN) that associated with unclear observation feature. This method was worked on special dataset with significant data volume that could be feasible for obtaining different input images based on morphological operators on them. This method is comparatively better than existing that provides effective performance in terms of DBN. But the system performance related to accuracy and false alarm attained are not up to the level to satisfy change detection model.

Using multiple detection fusion with a D-S evidence strategy, Hui Luo et al. [18] have presented a unique method for identifying the urban variability for very high resolution (VHR) pictures. In this study, we provide careful consideration to three methods for creating candidate change maps: interactive ISFA, Change Vector Analysis (CVA), and

International Journal on Recent and Innovation Trends in Computing and Communication
ISSN: 2321-8169 Volume: 11 Issue: 2
DOI: https://doi.org/10.17762/ijritcc.v11i2.6132
***Article Received**: 22 December 2022 **Revised**: 08 January 2023 **Accepted**: 26 January 2023*

iteratively reweighted multivariate alteration detection (IRMAD). The final transformation search result was derived from a study of three proofs, including the D-S proof and split object budget maps. Therefore, its superior performance is demonstrated by an analysis of search rate, comprehensive indicators, and false alarm rate. An unique multisensory, multi-temporal machine-learning strategy based on remote sensing big data for the finding of archaeological dunes in Cholistan has been introduced in the year 2020 by Hector a. Orango et al., [19]. (Pakistan). Many Indus Valley sites may be found in the Cholistan desert (ca. 3300 to 1500 BC). Cholistan's water shortages, the growth and fall of the Indus Valley Civilization, and the transition of the rich monsoon alluvial plains into very parched borders may all be pinned down to this one site. This technique used a machine learning strategy that used several data sources from different times periods to remotely examine archaeological mounds. The Google Earth engine has been updated with a classified algorithm that uses a massive database of artificial-hole radar and multispectral photos to provide a precise probability map for mound-like signals across an area of around 36,000 km 2. The key relevance for figuring out the area's archaeological significance is that the data suggest the area comprises a lot more ancient mounds than previously recorded, stretching south and east into the desert. Mounds ranging in size from less than five hectares to more than thirty hectares point to a dynamic habitation environment. This shift probably reflects the reactions of fluid hydrological networks and the gradual northward effect of the desert through time, which was eventually abandoned during the Harappan period.

III. Motivation & Problem Statement

The purpose of the change detection is to identify changed and unchanged regions in the same geographic area but by multi-temporal remote sensing images obtained at diverse times. The goal of replacing traditional search in multi-temporal images is to locate and analyze regions of land cover variation on the Earth's surface. By analyzing the multi-spectral information, the effective target detection and change detection can be processed. For this analysis several techniques are developed based on machine learning technique to detect changes in land cover. Such techniques are relying on labelling but it is difficult to perform on excessive or proper fitting for invasive changes. This method is based on support vector machine for enhancing the classification with supervisory learning approach. Here, the hyperplane is discovered with the help of optimizing this algorithm which clearly classifies the data point by incorporating the information of the composition with a given ground truth or labels. Still, for the best hyperplane requires well developed feature extraction and feature selection techniques. For these three types of techniques mentioned above, they cannot be widely used for changing investigative tasks due to their own limitations. Lots of methods are existed in change detection to attain the classification of unchanged and changed districts. But it obtaining minimum robustness because of the noise sensitivity and repeatedly ignoring the relationship between feature components. Therefore, it is very hard to attain better detection results. Inspired by this motivation, salient information of images is employed by integrating semantic change detection model to solve the problem that alteration images are often sensitive to noise corruption and light alteration.

IV. Proposed Semantic Change Detection Model

Change detection is an essential task from the multi temporal satellite images. To design Semantic Change Detection Deep Belief Neural Network (SCD-DBN) to locate and detect the changes with the consideration of feature pairs achieved from modules of widely various structures that involve various spatial ranges and parameter in quantities to factor in the discrepancy across various land cover distributions. To enhance the training process of DBN, the Jellyfish Algorithm (JA) is designed. The overall architecture of the projected perfect is offered as follows,

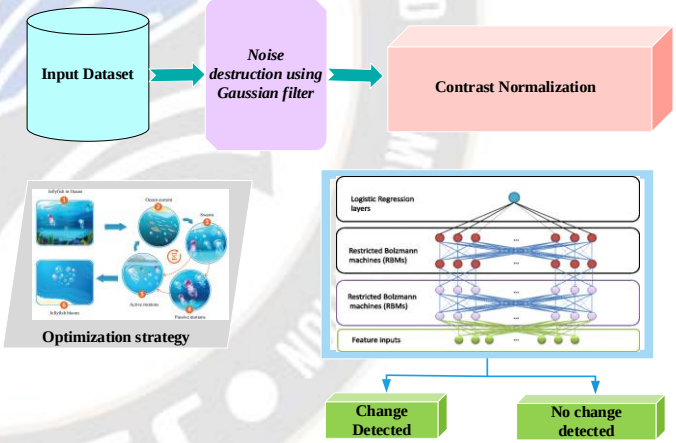

Figure 1: Overall Architecture of the projected model

The projected method is validated with the help image database especially multi-spectral images. The well-known database of Semantic Change detection Dataset (SECOND) is selected in this validation purpose. In the training and evaluation process of the proposed classifier, accuracy coefficient is utilized to alleviate the influences of label imbalance issues. The proposed classifier is validated by using MATLAB platform, performance analysis and comparison analysis. The proposed classifier is compared with existing algorithms.

International Journal on Recent and Innovation Trends in Computing and Communication
ISSN: 2321-8169 Volume: 11 Issue: 2
DOI: https://doi.org/10.17762/ijritcc.v11i2.6132
***Article Received**: 22 December 2022 **Revised**: 08 January 2023 **Accepted**: 26 January 2023*

4.1. Noise Destruction using Gaussian Filter

Multi-Spectral image J(y,z) taken from Semantic Change detection In order to reduce the amount of noise in the dataset, we use a Gaussian Filter to smooth out the image. It aids in enhancing the clarity of the image's edges. The following notation is a mathematical expression of this.

$$I_1(y,z) = J(y,z) * \frac{e^{\frac{-(y^2+z^2)}{2\sigma^2}}}{\sum_y \sum_z e^{\frac{-(y^2+z^2)}{2\sigma^2}}}, \quad \sigma = 2 \qquad (1)$$

For this application, we have set the sigma of the Gaussian filter to 2. The significance level (sigma) of 2 was chosen because smaller sigma values are confined to the immediate vicinity. However, if a large sigma value is chosen, the intracellular grey values will have a greater impact on the global background change. The resultant image enhances the performance of detection model by diminishing the disruptive factor and effect of noisy contents present in the image.

4.2. Image Enhancement using Contrast Normalization Approach

Generally, input multi-spectral images are captured under dissimilar remote sensors and may be prepared with different time period so that its illumination varies. This leads to input images of varying intensity and contrast that impede the performance and learning ability. Also, it is very hard to detect changed regions because of minimum level of contrast. In order to overcome this challenge Contrast Normalization (CN) is applied to avoid the contrast variation among filtered images. It is clearly explaining that the visual effects of changed region is enhanced by the saliency enhancement and is done by means of the proposed normalization function. For each and every image, primarily mean and standard deviation are computed. After calculating both, mean value is subtracted from the filtered image and dividing by its estimated standard deviation. The CN phase is evaluated by the subsequent mathematical expression.

$$N(y,z) = \frac{I_1(y,z)-\mu}{\sigma} \qquad (2)$$

Where N(y,z) designates the normalized image, I_1 (y,z) represents the filtered outcome, μ symbolizes the estimated mean value and σ denotes the standard deviation of an original image. With the help of proposed contrast normalization phase, the adaptability of the proposed model is wired. In addition, CN helps to diminish the effect of contrast variation during training of classification model among images.

4.3. Proposed Semantic Change Detection Deep Belief Network (SCD-DBN) in Multi-Spectral Image

Change detection tasks are performed by utilizing various techniques based on DL that are widely applied and which are driven by the change detection. More recently, a deep belief neural network (DBN) can automatically learn a complex feature space from a large amount of image data without heuristic feature extractions. The proposed change detection system is carried out using DBN model for detecting changes occurring in an environmental condition with dissimilar time series. Several Restricted Boltzmann Machines are stacked to form this energy-based probability generation model. It is implemented in a layer-by-layer fashion and includes two stages: training and testing. In this instance, the DBN layers are trained using a set of previously trained RBM layers. The first layer is the input and the second is the hidden layer, which houses the neurons. Edges connect the two layers, although communication between neurons within the same layer is blocked. The enclosing visible layer is shown here as

$$vis = \{vis_1, vis_2, \dots, vis_j, \dots, vis_m\};\ (vis_j \in \{0,1\}) \qquad (3)$$

Likewise, any one of the hidden layers employed in DBN is expressed as

$$hid = \{hid_1, hid_2, \dots, hid_j, \dots, hid_m\};\ (hid_j \in \{0,1\}) \qquad (4)$$

The layer that can be seen is denoted by the vis notation, while the layer that cannot is written as hid. The proposed CN method uses the input pre-processed result N(y,z) as a basis for defining the number of visible layers. These standard deviation-adjusted features are conveyed to the visible layer, from which they may be sent on to the concealed layer. Neurons in different layers are not directly connected to one another, but instead are linked via a weight connection between the two layers. This architecture has three initial parameters defined as =W,b,c>>. Here, W stands for the weight matrix, B stands for the hidden layer bias, and C stands for the visible layer bias. The proposed RBM architecture has n hidden neurons and m input neurons, where vis j denotes the visible unit in the jth layer and hid j represents the hidden unit in the jth layer. The mathematical form of the parameter structure is given in the following equation.

$$W = \{w_{j,k} \epsilon S^{m \times n}\} \qquad (5)$$

Here $w_{j,k}$ signifies weight value of noticeable and hidden neuron in j^{th} layer and k^{th} layer. The bias function of hidden layer B is exactly articulated as shadows.

$$B = \{b_j \epsilon S^n\} \qquad (6)$$

In the above equation, b_j term signifies a threshold for the bias function of the jth hidden neuron in the hidden layer. The visible layer's bias function is calculated in the same way.

$$C = \{c_k \epsilon S^m\} \qquad (7)$$

The c k term in the above equation represents the threshold value of the bias function for the kth visible neuron in the layer. Probability functions are learned between the hidden and the visible layers of an RBM using the energy function. The

International Journal on Recent and Innovation Trends in Computing and Communication
ISSN: 2321-8169 Volume: 11 Issue: 2
DOI: https://doi.org/10.17762/ijritcc.v11i2.6132
***Article Received**: 22 December 2022 **Revised**: 08 January 2023 **Accepted**: 26 January 2023*

probability distribution can be got by solving the subsequent equation for the energy function.

$$E(vis, hid|\theta) = -\sum_{j=1}^{m} b_j vis_j - \sum_{k=1}^{n} c_k hid_k - \sum_{j=1}^{m}\sum_{k=1}^{n} vis_j W_{jk} hid_k \quad (8)$$

Here $\theta = \{W_{jk}, b_j, c_k\}$ consist of the RBM model's parameters and the E term, which characterizes the energy function between the nodes in the hidden and the exposed layers. Similarly, the sum of m and n represents the total sum of exposed and concealed neurons, respectively.

In the next step, the probability function will be defined, taking into account the energy function's exponential and regularization. The following is a mathematical expression of the joint probability distribution of the RBM model between the exposed and concealed layers.

$$P(vis, hid|\theta) = \frac{1}{Z(\theta)} e^{-E(vis,hid|\theta)} \quad (9)$$

This equation derives from the Gibbs distribution function of the RBM model. This equation is the basis for deriving the partition function:

$$Z(\theta) = \sum_{vis,hid} e^{-E(vis,hid|\theta)} \quad (10)$$

Here $Z(\theta)$ The phrase denotes a distributed or normalized function representing the overall energy status of all layers, both those that are immediately apparent and those that are not. It's produced by adding together the results of the energy assessment performed on the visible layer and the hidden layer. The parameter values can be acquired by calculating a probability function. In this case, the notation is the primary tool for formulating the overall distribution of both visible and hidden layers in concert $P(vis, hid|\theta)$. Then the marginal distribution function of visible layer is intended using $P(vis|\theta)$ and can be mathematically labeled as follows.

$$P(vis|\theta) = \frac{1}{Z(\theta)} \sum_{hid} e^{-E(vis,hid|\theta)} \quad (11)$$

Summarizing the whole network criteria allows us to assess the above marginal distribution function of the visible layer. The following equation is used to derive the hidden layer's marginal distribution function.

$$P(hid|\theta) = \frac{1}{Z(\theta)} \sum_{vis} e^{-E(vis,hid|\theta)} \quad (12)$$

Due to its exponential shape, the RBM architecture supports connections between layers as well as connections inside each layer. In addition, RBM's exposed and concealed layers are autonomous, therefore its conditional probability values can be calculated using the following formulas.

$$P(vis|hid) = \prod_j P(vis_j|hid) \quad (13)$$

$$P(hid|vis) = \prod_k P(hid_k|vis) \quad (14)$$

Since the suggested RBM construction is made up of components in a binary state, the activation function to be used is a sigmoid one, as exposed below.

$$sigmoid(y) = \frac{1}{(1+e^{-y})} \quad (15)$$

Probability of RBM structure's activation function for both the visible and hidden layers is formulated based on the preceding activation function, and it is given as follows.

$$sigmoid(y) = \frac{1}{(1+e^{-y})} \quad (16)$$

$$P(vis_j = 1|hid) = \frac{1}{1+exp(-b_j - \sum_{k=1}^{n} w_{jk} hid_k)} \quad (17)$$

$$P(hid_k = 1|vis) = \frac{1}{1+exp(-c_k - \sum_{j=1}^{m} w_{jk} vis_j)} \quad (18)$$

Updating the rules for the involved parameters = W,b,c is the next step in the proposed categorization framework. There are cases where the RBM model's Gibbs distribution function cannot be implemented in the shortest possible time. Because of this, we recommend a fast-learning technique called Contrast Divergence (CD) to help reduce the amount of time needed for such tasks. The below equations mathematically present the revised parameter values based on the aforementioned learning strategy.

$$W^{time+1} = W^{time} + \varepsilon\left(P(hid|vis^{(0)})[vis^{(0)}]^{time} - P(hid|vis^{(1)})[vis^{(1)}]^{time}\right) \quad (19)$$

$$b^{time+1} = b^{time} + \varepsilon(vis^{(0)} - vis^{(1)}) \quad (20)$$

$$c^{time+1} = c^{time} + \varepsilon\left(P(hid|vis^{(0)}) - P(vis^{(1)})\right) \quad (21)$$

Here, time signifies the iterative step size and is the rate of learning. The preceding steps are iterated upon until the parameter values have been modified to produce a feature representation that is both more abstract and more representable than the one produced by the lower layer. The proposed model successfully attained its goal of feature extraction by utilizing the aforementioned equations. Because of the training technique utilized by the jellyfish optimization procedure, the proposed change detection model can sidestep difficult functionalities. As a result, the overall process yields a more advanced feature set, which improves the detection system's efficiency.

4.3.1 Training SCD-DBN Model with Jellyfish algorithm

In the DBNN, the learning rate is optimally designated with the help of Jellyfish procedure. The detail explanation of the optimization algorithm is presented in this section. In general, Jellyfish live in the water of various temperatures and depths around the world and its search behavior is inspired by scholars to frame the optimization model. With its hunting behavior, optimization technique is defined in our research work to train the proposed SCD-DBN network model for tuning learning rate. The jellyfish algorithm is exactly formulated as three perfect rules,

- It's possible that jellyfish will follow the school and the current if they're in the water. In order to organize, this movement is shifting between the two processes.

International Journal on Recent and Innovation Trends in Computing and Communication
ISSN: 2321-8169 Volume: 11 Issue: 2
DOI: https://doi.org/10.17762/ijritcc.v11i2.6132
Article Received: 22 December 2022 Revised: 08 January 2023 Accepted: 26 January 2023

- Jellyfish will go where there is food, thus they will swim around the ocean floor. Where they are larger in number depends on where you look.
- To determine how much food to provide, we consider the relevant objective function and geographic location.

The jellyfish algorithm is obtainable in the upcoming steps.

Ocean Current

Jellyfishes thrive and are drawn to the ocean current due to the high concentration of nutrients in it. We determine the ocean current direction by taking the mean of the vectors from all of the jellyfish in the ocean to the jellyfish that is currently in the best position. What follows is the formula for the jellyfish current in the ocean:

$$\overrightarrow{O.C} = \frac{1}{Pop^N}\sum(X^* - E^c X^i) = X^* - E^c\frac{\sum X^i}{Pop^N} = X^* - E^c\mu \quad (22)$$

Set $df = E^c\mu$,

Hence, the ocean current is computed based on below equation,

$$\overrightarrow{O.C} = X^* - df \quad (23)$$

Where, df can be expressed as the average distance between the best and average locations of the jellyfish, where is the average location of the jellyfish, Ec is the attraction factor, X* is the optimal location of the jellyfish, and N is the population size. If we assume a uniform three-dimensional distribution of jellyfish, then the probability that every given jellyfish is located at a given distance from its mean location is unambiguous. Following is a mathematical expression for the jellyfish's distance:

$$D = \pm\beta\sigma \quad (24)$$

$$df = \beta \times \sigma \times rand^f(0,1) \quad (25)$$

$$\sigma = rand^\alpha(0,1) \times \mu \quad (26)$$

The novel optimal location of jellyfish is obtainable as,

$$X^i(T+1) = X^i(t) + rand(0,1) \times \overrightarrow{O.C} \quad (27)$$

***Jellyfish* swarm**

It is possible to classify jellyfish behavior into two distinct categories: active and passive. The local search or exploitation can be treated using the below formulas, which are based on the jellyfish's movements.

$$\vec{s} = X^i(t+1) - X^i(t) \quad (28)$$

From the above equation, the calculation is obtainable as shadows,

$$\vec{s} = rand(0,1) \times \vec{D} \quad (29)$$

$$\vec{D} = \begin{cases} X^j(t) - X^i(t) \ \ if\ f(X^i \geq fX^j) \\ X^i(t) - X^j(t)\ if\ \ f\ (X^i < fX^j) \end{cases} \quad (30)$$

Where, f is labeled as an objective function of location.

Initial Population

The jellyfish population is initially generated at random. As a result of slow convergence and being stuck at local optima, the jellyfish could be negatively impacted. It's possible that the low diversity of the population is to blame for the slow convergence. There are a variety of chaotic maps out there, including the tent map and the logistic map, that were developed to speed up the previously slow convergence rate. One of the most elementary chaotic maps, the logistic map, is chosen. Initiating populations with this map was more diverse than with random assortment. Therefore, the logistical diagram looks like this:

$$X^{i+1} = \eta X^i(1 - X^i),\ \ 0 \leq X^0 \leq 1 \quad (31)$$

Where, X^0 can be described as jellyfish $X^0 \epsilon (0,1)$ and X^i is described as logistic chaotic value of location. The parameter is set as 4.0.

Boundary Conditions

The distribution and abundance of jellyfish are largely determined by the specifics of different oceans. The jellyfish boundary conditions are as follows,

$$\begin{cases} X_{ref}^{i,d} = (X^{i,d} - U^{u,d}) + L^b(d)\ if\ X^{i,d} > U^{b,d} \\ X_{ref}^{i,d} = (X^{i,d} - L^{b,d}) + U^b(d)\ if\ X^{i,d} < U^{b,d} \end{cases} \quad (32)$$

Where, $L^{b,d}$ can be described as lower bound restraints in search space, $U^{u,d}$ is labeled as upper bound constraints in search space and $X^{i,d}$ can be labelled as jellyfish location.

Fitness Calculation

The fitness function is calculated after the initial population is complete. The optimal SCD-DBN learning rate is based on the fitness function. We take into account the error function when assessing the fitness function. Achieving the fitness function requires determining the best possible learning value. This is the mathematical version of the fitness function:

$$F = \min\{\text{MSE}\} \quad (33)$$

$$MSE = \frac{1}{N*M}\sum_{X=1}^{N}\sum_{Y=1}^{M}\left[I_{image}(A,B) - I_{d-image}(A,B)\right]^2 \quad (34)$$

Where, $I_{d-image}(A,B)$ is described as changed images and $I_{image}(A,B)$ is described as input image. Based on the fitness

International Journal on Recent and Innovation Trends in Computing and Communication
ISSN: 2321-8169 Volume: 11 Issue: 2
DOI: https://doi.org/10.17762/ijritcc.v11i2.6132
***Article Received**: 22 December 2022 **Revised**: 08 January 2023 **Accepted**: 26 January 2023*

purpose, the optimal learning values are selected which used to enhance the proposed network model.

V. Results and Discussion

The results of experiments conducted on the suggested semantic change detection system are shown here. Classification Accuracy, Recognition Error, Sensitivity, Specificity, MCC, and Processing Time are only few of the assessment metrics used to prove the efficacy of the suggested system. True positives, false negatives, false positives, and false positives are all calculated by the confusion matrix (False Negative). Here, we use 80% of the photos in the dataset for training purposes, and the remaining 20% for evaluation.

5.1 Dataset Description

This paper introduced SECOND, a comprehensive change detection dataset, with the goal of establishing a new standard for change detection problems with sufficient quantities, sufficient categories, and proper annotation approaches. First, gather 4662 pairs of aerial photos from various platforms and sensors to guarantee data diversity. Cities like Hangzhou, Chengdu, and Shanghai are all represented by these paired photographs. Each image is 512 pixels on the longest side and has pixel-level annotations. An experienced team of earth vision apps annotates SECOND, ensuring precise labelling. There are six primary land-cover classes to consider when analyzing the SECOND dataset's change category: non-vegetated ground surface, tree, low vegetation, water, buildings, and playgrounds. Specifically, in the new data set, impervious surface and bare land correspond to non-vegetated ground surface (surface, for short). In conclusion, the combination of these 6 land-cover types yields 30 distinct change types (including non-change). By picking image pairs at random, SECOND accurately portrays how land-cover categories are distributed in response to changes.

5.2. Performance Outcome of Proposed Model

The following figure depicts the accuracy and loss function obtained by the detection system after implementing the proposed SCD-DBN method.

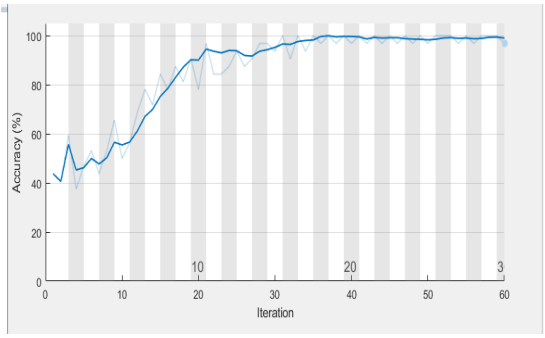

Figure 2: Simulation consequence of accuracy measure

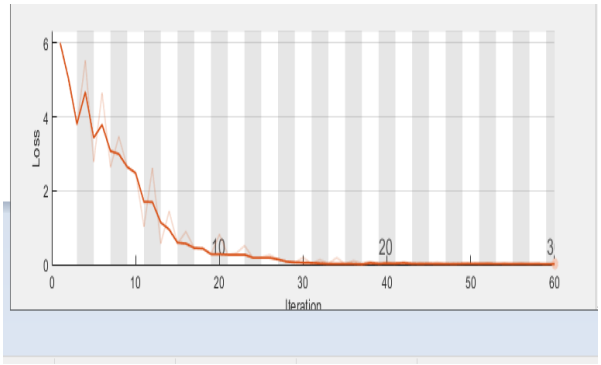

Figure 3: Simulation result for prediction system loss function

Figures 2 and 3 show that the suggested SCD-DBN method yields high accuracy in the semantic change detection system. Calculating both accuracy and loss function yields useful information, with loss function defining the prediction error attained by the projected system. As the number of iterations is raised, for instance, so is the resulting accuracy. However, the prediction error of the projected solution decreases when the sum of iterations is increased. As a result, it excels in comparisons of accuracy and error function. In the following sections, we compare and analyze the proposed methodology in light of previously used methods.

5.3. Overall Comparison Analysis of Proposed and Existing Techniques

The proposed system SCD-DBN with optimization model is compared with existing techniques like Naive Bayes, Artificial Neural Network (ANN), Decision Tree, random Forest, Pre-trained CNN.

TABLE I: Performance Assessment of Proposed and Eexisting Prediction System

Detection model	**Classifier Performance**					
	Accuracy (%)	*Specificity (%)*	*Sensitivity (%)*	*MCC*	*Time(s)*	*Error*
Naive Bayes	82.6	86.91	77.3	0.4	19.438	0.92
ANN	75.12	72.78	74.29	0.476	20	0.98
Decision Tree	75.04	77.43	66.97	0.56	22.61	0.9
Random Forest	82	70.1	95.38	0.805	17.89	0.82
SVM	77	79.9	86.5	0.42	34	0.86
Pre-trained CNN	89.90	85	94.59	0.7	13.96	0.69
SCD-DBN	**94.07**	**95.00**	**98.64**	**96.79**	**9.71**	**0.34**

In Table 1, we can see how deep learning stacks up against machine learning on the change detection dataset as a whole. The proposed strategy significantly decreases the error function and the processing time. Other metrics, such as accuracy, sensitivity, specificity, and MCC, are also improved for the

International Journal on Recent and Innovation Trends in Computing and Communication
ISSN: 2321-8169 Volume: 11 Issue: 2
DOI: https://doi.org/10.17762/ijritcc.v11i2.6132
***Article Received**: 22 December 2022 **Revised**: 08 January 2023 **Accepted**: 26 January 2023*

sampled data. It is clear that the suggested SCD-DBN achieves 94.07% accuracy, while the default CNN model achieves 89.9%, the SVM achieves 77%, and both the Navier-Stokes and Random Forest algorithms achieve around 82%. Furthermore, the proposed method has a sensitivity of 95.00% and a specificity of 98.64%. It appears that the outcomes of these two measurements are superior to those of currently used alternatives.

VI. CONCLUSION

The proposed method is validated with the help image database especially multi-spectral images. Designing Semantic Change Detection Deep Belief Neural Network (SCD-DBNN) to locate and detect the changes with the consideration of feature pairs achieved from modules of widely various constructions, that involve various spatial ranges and parameter in quantities to factor in the discrepancy across various land cover deliveries. To enhance the training process of DBNN, the Jellyfish Algorithm (JA) is designed. The well-known database of Semantic Change detection Dataset (SECOND) is selected in this validation purpose. In the training and evaluation process of the proposed classifier, accuracy metric is utilized to alleviate the influences of label imbalance issues. The proposed classifier is validated by using MATLAB platform, performance analysis and comparison analysis.

REFERENCES

[1] Luppino, L.T., Kampffmeyer, M., Bianchi, F.M., Moser, G., Serpico, S.B., Jenssen, R. and Anfinsen, S.N., 2021. Deep image translation with an affinity-based change prior for unsupervised multimodal change detection. IEEE Transactions on Geoscience and Remote Sensing.

[2] Alonso-Arévalo, M.A., Cruz-Gutiérrez, A., Ibarra-Hernández, R.F., García-Canseco, E. and Conte-Galván, R., 2021. Robust heart sound segmentation based on spectral change detection and genetic algorithms. Biomedical Signal Processing and Control, 63, p.102208.

[3] De Kerangal, M., Vickers, D. and Chait, M., 2021. The effect of healthy aging on change detection and sensitivity to predictable structure in crowded acoustic scenes. Hearing Research, 399, p.108074.

[4] Banerjee, T., Gurram, P. and Whipps, G., 2021. A Bayesian theory of change detection in statistically periodic random processes. IEEE Transactions on Information Theory.

[5] Chen, S., Yang, K. and Stiefelhagen, R., 2021. DR-TANet: Dynamic Receptive Temporal Attention Network for Street Scene Change Detection. arXiv preprint arXiv:2103.00879.

[6] Seydi, S.T., Hasanlou, M. and Amani, M., 2020. A new end-to-end multi-dimensional CNN framework for land cover/land use change detection in multi-source remote sensing datasets. Remote Sensing, 12(12), p.2010.

[7] Ma, L., Zhenhong, J., Yang, J. and Kasabov, N., 2020. Multi-spectral image change detection based on single-band iterative weighting and fuzzy C-means clustering. European Journal of Remote Sensing, 53(1), pp.1-13.

[8] Wiratama, W., Lee, J. and Sim, D., 2020. Change detection on multi-spectral images based on feature-level U-Net. IEEE Access, 8, pp.12279-12289.

[9] Han, H., Han, C., Lan, T., Huang, L., Hu, C. and Xue, X., 2020. Automatic shadow detection for multispectral satellite remote sensing images in invariant color spaces. Applied Sciences, 10(18), p.6467.

[10] Khusni, U., Dewangkoro, H.I. and Arymurthy, A.M., 2020, September. Urban Area Change Detection with Combining CNN and RNN from Sentinel-2 Multispectral Remote Sensing Data. In 2020 3rd International Conference on Computer and Informatics Engineering (IC2IE) (pp. 171-175). IEEE.

[11] Wang, M., Tan, K., Jia, X., Wang, X. and Chen, Y., 2020. A deep siamese network with hybrid convolutional feature extraction module for change detection based on multi-sensor remote sensing images. Remote Sensing, 12(2), p.205.

[12] Shi, W., Zhang, M., Zhang, R., Chen, S. and Zhan, Z., 2020. Change detection based on artificial intelligence: State-of-the-art and challenges. Remote Sensing, 12(10), p.1688.

[13] Chen, H. and Shi, Z., 2020. A spatial-temporal attention-based method and a new dataset for remote sensing image change detection. Remote Sensing, 12(10), p.1662.

[14] Jameel, S.M., Hashmani, M.A., Rehman, M. and Budiman, A., 2020. Adaptive CNN ensemble for complex multispectral image analysis. Complexity, 2020.

[15] Peng, D., Zhang, Y. and Guan, H., 2019. End-to-end change detection for high resolution satellite images using improved UNet++. Remote Sensing, 11(11), p.1382.

[16] Mou, L., Bruzzone, L. and Zhu, X.X., 2018. Learning spectral-spatial-temporal features via a recurrent convolutional neural network for change detection in multispectral imagery. IEEE Transactions on Geoscience and Remote Sensing, 57(2), pp.924-935.

[17] Samadi, F., Akbarizadeh, G. and Kaabi, H., 2019. Change detection in SAR images using deep belief network: a new training approach based on morphological images. IET Image Processing, 13(12), pp.2255-2264.

[18] Luo, H., Liu, C., Wu, C. and Guo, X., 2018. Urban change detection based on Dempster–Shafer theory for multitemporal very high-resolution imagery. Remote Sensing, 10(7), p.980.

[19] Orengo, H.A., Conesa, F.C., Garcia-Molsosa, A., Lobo, A., Green, A.S., Madella, M. and Petrie, C.A., 2020. Automated detection of archaeological mounds using machine-learning classification of multisensor and multitemporal satellite data. Proceedings of the National Academy of Sciences, 117(31), pp.18240-18250.

[20] Liu, L., Wang, J., Zhang, E., Li, B., Zhu, X., Zhang, Y. and Peng, J., 2020. Shallow–deep convolutional network and spectral-discrimination-based detail injection for multispectral imagery pan-sharpening. IEEE Journal of Selected Topics in Applied Earth Observations and Remote Sensing, 13, pp.1772-1783.